Structural characterization of an α-1, 6-linked galactomannan from natural *Cordyceps sinensis*

Junqiao Wang [a], Shaoping Nie [a], Shuping Chen [a], Aled O. Phillips [b], Glyn O. Phillips [c], Yajing Li [d], Mingyong Xie [a*], Steve W. Cui [a,e]

[a] *State Key Laboratory of Food Science and Technology, Nanchang University, 235 Nanjing East Road, Nanchang, Jiangxi Province, 330047, China*

[b] *School of Medicine, University of Cardiff, Wales, UK*

[c] *Phillips Hydrocolloids Research Centre, Glyndwr University, Wrexham, LL11 2AW Wales, UK*

[d] *Qinghai Ta Er Sheng Gu Agricultural Science and Technology Co. Ltd., Xining 810003, China*

[e] *Guelph Research and Development Centre, Agriculture and Agri-Food Canada, 93 Stone Road West, Guelph, Ontario, N1G 5C9, Canada*

* Corresponding authors:

myxie@ncu.edu.cn (Professor Mingyong Xie, PhD), Tel. & Fax: +86-791-83969009.

Steve.Cui@agr.gc.ca (Professor Steve W. Cui, PhD),Tel.: +1-5197808028; Fax: +1-5198292600.

Abstract

An α-1, 6-linked galactomannan was isolated and purified from natural *Cordyceps sinensis*. The fine structure analysis of this polysaccharide was elucidated based on partial acid hydrolysis, monosaccharide composition, methylation and 1D/2D nuclear magnetic resonance (NMR) spectroscopy. Monosaccharide composition analysis revealed that this polysaccharide was mainly composed of galactose (68.65%), glucose (6.65%) and mannose (24.02%). However, after partial acid hydrolysis the percentages of galactose, glucose and mannose were changed to 3.96%, 13.82% and 82.22%, respectively. The molecular weight of this polysaccharide was 7207. Methylation and NMR analysis revealed that this galactomannan had a highly branched structure, mainly consisted of a mannan skeleton and galactofuranosyl chains. The structure of galactofuranosyl part was formed by alternating (1→5)-lined β-Gal*f* and (1→6)-liked β-Gal*f* or a single (1→6)-liked β-Gal*f*, attaching to the *O*-2 and *O*-4 of the mannose chain, and terminated at β-T-Gal*f*. The mannan core was revealed by analyzing the partial acid hydrolysate of the galactomannan and the structure was composed of (1→6)-linked α-Man*p* backbone, with substituted at C-2 by short chains of 2-substituted Man*p* or Gal*f* branches.

Key words: natural *Cordyceps sinensis*; low molecular weight polysaccharide; alkali extraction; structure

1. Introduction

Cordyceps sinensis (Berk.) Sacc., called "DongChongXiaCao" in Chinese, is a valued Chinese caterpillar fungus that has been extensively used as tonic and medicinal food for more than 700 years. It was mainly distributed in the prairie soil at altitudes of above 3500 meters in the Qinghai-Tibetan Plateau. *C. sinensis* has a wide-range of nutritional and pharmacological benefits on the immune, circulatory, cardiovascular, hematogenic and respiratory systems (Chen, Wang, Nie, & Marcone, 2013). These beneficial effects might be attributed to a number of bioactive compounds that has been detected in *C. sinensis*, including polysaccharide, amino acids, fatty acids, minerals, mannitol and nucleoside (Wang, et al., 2015). Among them, the polysaccharide had been widely studied for their potent activities such as anti-tumor, antioxidant, immunomodulatory, hypoglycemic, *etc.* (Nie, Cui, Xie, Phillips, & Phillips, 2013).

The polysaccharide is mainly presented in the walls of the fungal cells. It was reported that the fungal cell wall is composed of two major kinds of polysaccharides, a rigid fibrillary of chitin (or cellulose) and a matrix-like glucan or glycoproteins (Zhang, Cui, Cheung, & Wang, 2007). Besides, a small proportion of water-soluble galactomannan was also found in the surface of fungal wall using dilute alkali extraction (Leal, Prieto, Bernabé, & Hawksworth, 2010). In most cases, the chemical structure of these galactomannans was similar, with a mannan backbone and branching galactosyl residues as the common units. In our previous study, we have characterized the structure of a bioactive hydrophilic glucan (CBHP) from *C. sinensis*, which was comprised a main chain of α-1,4- Glc*p* and α-1,3-Glc*p*, and a side chain of α-T-Glc*p*, with branching point at O-2 or O-6 (Nie, et al., 2011). To date, the galactomannan structure has been also revealed in *C. sinensis*, but not very commonly reported. In early 1977, Miyazaki *et al*. reported a purified galactomannan, CS-I, from ascocarps of *C. sinensis*, consisting of mannan chain with α-1,2- Man*p* residues and galactosyl oligomer containing branches (Miyazaki, Oikawa, & Yamada, 1977). Using 5% sodium carbonate extraction, Kiho *et al*. obtained a water-soluble, minor protein-containing galactomannan (CT-4N), which mainly consisted of α-1,6- Man*p* and α-1,2- Man*p* in the main chain and a large proportion of β-1,5-Gal*f* in the branches (Kiho, Tabata, Ukai, & Hara, 1986). However, the detailed structure of these galactomannans has not yet been achieved.

Therefore, in order to obtain a comprehensive knowledge of the polysaccharides from *C. sinensis*,

we successfully separated a highly purified galactomannan from the water-insoluble residues of natural *C. sinensis* and further characterized the chemical structure of this polysaccharide by molecular weight, monosaccharide composition, methylation, partial acid hydrolysis and 1D/2D NMR spectroscopy.

2. Materials and Methods

2.1. Materials

The dried natural *C. sinensis* was collected from Qinghai province, China. Monosaccharide standards, including fucose (Fuc), rhamnose (Rha), arabinose (Ara), galactose (Gal), glucose (Glc), mannose (Man), xylose (Xyl), fructose (Fru), ribose (Rib), galacturonic acid (GalA) and glucuronic acid (GlcA) were purchased from Sigma-Aldrich (St. Louis, MO, USA). Deuterium oxide (D_2O) and sodium borodeuteride ($NaBD_4$, 98 atom % D) were from Acros Organics (New Jersey, USA). All the other reagents were of analytical grade unless specified.

2.2. Isolation and purification of the polysaccharide

The flowchart for the extraction and fractionation procedure was shown in **Fig. 1a**. Briefly, the powder of natural *C. sinensis* after exhaustively extracting with hot water was collected and dried. It was then extracted with 0.5 $mol \cdot L^{-1}$ NaOH/0.01 $mol \cdot L^{-1}$ $NaBH_4$ at 4 ºC two times, each for 12 h. After centrifugation, all the supernatant was collected and neutralized with 1 $mol \cdot L^{-1}$ HAc. The solution was then centrifuged again to separate the supernatant, achieving the alkali extraction water-soluble fraction. After dialysis and precipitation with ethanol, a crude polysaccharide was obtained. Subsequently, the protein was removed by Sevag method (chloroform/1-butanol, v/v = 4:1) and protease (Megazyme, Ireland) hydrolysis, and then dialysis and further froze dry to get the alkali-extractable polysaccharide from natural *C. sinensis*. The alkali-extractable polysaccharide was then fractionated and purified by precipitating with ethanol repeatedly, and the supernatant, the major fraction, was collected for the following analysis.

2.3. Partial acid hydrolysis

The polysaccharide (~45 mg) was hydrolyzed with 0.1 $mol \cdot L^{-1}$ TFA (10 mL) at 100 ºC for 0.5 h, 1 h and 2 h, respectively. After cooling to room temperature, the hydrolysates were dialyzed against distilled water for 48 h (molecular weight cut-off 3500). The solutions collected from both the inner and outside fractions of dialysis bag were concentrated and lyophilized, named as 0.5h-I/O, 1h-I/O

and 2h-I/O, respectively.

2.4. Purity and molecular weight distribution

The purity and molecular weight distribution of the polysaccharide and its hydrolysates were determined by HPSEC (Shimadzu SCL-10Avp, Shimadzu Scientific Instruments Inc., Columbia, MA, USA) with multiple detectors: a differential pressure viscometer (DP), a refractive index detector (RI), a UV detector, a right angle laser light scattering detector (RALLS) and a low angle laser light scattering detector (LALLS). Two columns in series, a PAA-M (Aqua Gel^{TM} Series, Polyanalytik Canada) and a PAA-203 (Aqua Gel^{TM} Series, Polyanalytik Canada) were used. The eluent was 0.1 mol·L^{-1} $NaNO_3$/0.02% NaN_3 aqueous solution at a flow rate of 0.5 mL/min. The temperature of columns, viscometers and RI detector was kept at 40 ºC. The dn/dc value was 0.146 mL/g. Polysaccharide and standard solutions were filtered through 0.45 μm filter prior to injection. Data was obtained and processed using the OmniSEC 4.6.1 software.

2.5. Monosaccharide composition

Monosaccharide composition of polysaccharides was determined by a complete-acid hydrolyzing in 2 mol·L^{-1} H_2SO_4 at 100 ºC for 2 h, followed by high performance anion exchange chromatography coupled with pulsed amperometric detection (HPAEC-PAD). Analysis of the polysaccharide was performed on Dionex ICS-5000 System (Dionex Corporation, CA) equipped with a CarboPac PA20 Guard (3 mm × 30 mm, Dionex, CA) and a CarboPac PA20 column (3 mm×150 mm, Dionex, CA), and separation was carried out under a gradient elution (2 mmol·L^{-1} NaOH eluted for 20 min, followed by adding NaOAc from 5% to 20% in 10 min) at a flow rate of 0.5 mL/min. On the other hand, measurements of the polysaccharide and its hydrolysates were recorded on Dionex ICS-500 System (Dionex Corporation, CA) fitted with a CarboPac PA1 column (3 mm×150 mm, Dionex, CA) using a separation condition reported by Nie, et al. (2011).

2.6. Glyosidic linkages

Methylation analysis was carried out according to the method of Ciucanu and Kerek (1984) with slight modification. Briefly, dried polysaccharide was stirred constantly overnight to make it completely dissolve in anhydrous DMSO. Subsequently, prior to reacting with methyl iodide, dried NaOH powder was added to make the polysaccharide solution in an alkaline environment. The methylated polysaccharide was obtained by extracting with dichloromethane and further detected

by infrared spectra to confirm a complete reaction. The dried methylated product was hydrolyzed by 4 $mol \cdot L^{-1}$ trifluoroacetic acid (TFA) in a sealed tube at 100 ºC for 6 h. Finally, the hydrolysate was reduced with $NaBD_4$ and acetylated with acetic anhydride to result partially methylated alditol acetates (PMAAs). The PMAAs were injected to a GC-MS system (Thermo 1310 GC-ISQ LT MS,) with a TG-5MS capillary column (60 m×0.25 mm, 0.25 μm film thickness, 160 ºC to 210 ºC at 2 ºC / min, then 210 ºC -240 ºC at 5 ºC / min) for analysis.

2.7. NMR spectroscopy

The galactomannan and its hydrolysate (2h-I) was exchanged with deuterium by lyophilizing against D_2O for three times and was finally dissolved in 0.7 mL D_2O, respectively, at room temperature before NMR analysis.

For analysis of the galactomannan, studies included ^{1}H, ^{13}C spectrum, correlation spectroscopy (COSY), heteronuclear single-quantum coherence (HSQC) and heteronuclear multiple-bond correlation (HMBC), and were conducted at 294 K. And for analysis of the hydrolysate (2h-I), all the experiments, including ^{1}H, ^{13}C spectrum, homonuclear $^{1}H/^{1}H$ correlation (COSY, TOCSY and NOESY), HSQC and HMBC were carried out at 313K. All experiments were recorded on a Bruker Avance 600 MHz NMR spectrometer (Brucker, Rheinstetten, Germany).

2.8. Statistical analysis

The data was obtained with triple replications and was presented in mean, and the statistical analysis was performed through statistical software (SPSS, Version 17.0).

3. Results and Discussion

3.1 Purification and molecular weight of the galactomannan

The crude polysaccharide was obtained from the dry water-insoluble residues of natural *C. sinensis* by cold alkali extraction and ethanol precipitation with a yield of approximately 1.91% ± 0.06 (w/w) of the total dried materials. Due to a high content of protein (39.11% ±0.17) as determined by total protein assay kit (Sigma-Aldrich, USA), it was then removed the protein by Sevag method and protease hydrolysis before processing to ethanol precipitation.

The molecular weight distribution of the galactomannan was determined by HPSEC. As shown in **Fig. 1b**, the galactomannan was eluted as a major and symmetrical peak from HPSEC, indicating that this galactomannan was a homogeneous polysaccharide. The molecular weight (Mw) of the

galactomannan was calculated to be 7207 using pullulan as standard. Mw/Mn was used to investigate the width of the molecular weight distribution, representing the dispersity of a polymer. The Mw/Mn for the galactomannan was estimated to be 1.2, indicating that the polysaccharide was a narrow-distributed polymer. The intrinsic viscosity of the polysaccharide was determined to be 0.032 dL/g, and the extreme low intrinsic viscosity might be attributed to its low molecular weight.

3.2 Partial acid hydrolysis and monosaccharide composition

The result of HPAEC-PAD analysis showed that the polysaccharide was mainly composed of galactose, glucose and mannose in an approximate percentage of 68.65%, 6.65% and 24.02%, with trace amount of rhamnose. The small amount of glucose might be the contamination of the water-extracted polysaccharide, which was found to be an α-,4-glucan (Wang, et al., 2017). In addition, no uronic acid was observed as detected on Dionex ICS-5000 System separated by CarboPac PA20 column (Supplemental Figure 1), indicating that the polysaccharide was a neutral polysaccharide.

Due to the structural complexity of polysaccharides, a partial acid hydrolysis process was employed to characterize the galactomannan. **Fig. 1b** showed the HPSEC elution profiles of the hydrolysates (the high molecular weight fragments) of the galactomannan. All the three fragments exhibited a major sharp and symmetrical peak similar to the galactomannan, demonstrating that the hydrolysis processes did not break up the main chain. It was worth noting that the retention volumes of the hydrolysates were increased gradually with the increase of hydrolysis duration. Generally, it was believed that the removal of branches was relative easier than that of the backbone of the polysaccharide during the acid hydrolysis, since the acid prior to break up the residues in the side chain or terminal of the polysaccharide. The increased of retention volumes suggested the effective removal of side chains without a significant influence on backbone of the galactomannan. On the other hand, it was interesting to find that the content of galactose in the inner side of dialysis bag corresponding to the relative high molecular weight fragment was significantly decreased to 22.17%, and further dropped to only around 2-3% as the hydrolysis duration extended to 1 h and 2 h (Table 1), indicating that the majority of galactose could be easily hydrolyzed by 0.1 M TFA. On the contrary, the percentage of mannose was increased dramatically to 70.66%, 89.66% and 82.22% after TFA treatment for 0.5 h, 1 h and 2 h, respectively. Unexpectedly, the result indicated that the mannose, instead of galactose, was likely to locate in the backbone of the galactomannan, while

most of the galactose might exist in the branches.

3.3 Methylation analysis

Further detailed information of glycosidic linkages for the galactomannan and its hydrolysate (2h-I) was investigated using methylation analysis coupled with GC-MS detection. Result suggested a fairly complex structure with around 15 types of linkage patterns (**Table 2**, listed in the order of retention time). Sugar residues, such as T-Gal*f*, 1,5-Gal*f*, 1,6-Man*p*, 1,6-Gal*f* and 1,2,6-Man*p*, were the major residues in the galactomannan. However, the percentages of T-Gal*f*, 1,5-Gal*f* and 1,6-Gal*f* were decreased significantly in the hydrolysate (2h-I), indicating these galactofuranosyl residues were easily to move away by the acid and thus might be located at the end of branches. On the contrary, 1,6-Man*p* increased dramatically to become the dominate sugar residue in the hydrolysate (2h-I), accounting for 51.98% of all the linkage patterns.

Degree of branching (DB) is an important parameter that reflects the structure of a polymer. If the value of DB equals to 0, it indicates that the polymer has a linear chain without any branches, but for a fully branched structure, the number is 1 (Guo, et al., 2015). The DB for the galactomannan and its hydrolysate (2h-I) was calculated to be 0.55 and 0.34, respectively, according to equation reported by (Qian, Cui, Nikiforuk, & Goff, 2012), suggesting that the galactomannan had a highly branched structure, but less branched after partial acid hydrolysis. Therefore, combined with the results of monosaccharide composition and methylation analysis, we deduced that the main chain of the galactomannan might be composed of 1,6-Man*p* mainly branching at O-2, and the terminal sugar residues might be including T-Gal*f*, T-Man*p*, as well as the small percentage of T-Glc*p* and T-Gal*p*.

3.4 NMR spectroscopy analysis of the galactomannan

The ^{1}H NMR spectrum (**Fig. 2a**) of the galactomannan showed a complex pattern of signals in the anomeric region, since more than ten peaks were detected. Among them, three major (5.15, 4.96 and 4.94 ppm) and four minor (5.07, 5.06, 4.99 and 4.83 ppm) anomeric signals were found to be significant and were used for analysis. In ^{13}C NMR spectrum (**Fig. 2b**), the dominant anomeric signals were centered at 108.12 ppm and 107.26 ppm, indicating the presence of β-galactofuranosyl residues because of the obvious low field. Meanwhile, six minor peaks (106.13, 101.24, 100.84, 99.84, 98.38 and 97.35 ppm) were also observed. From the HSQC spectrum (**Fig. 2d**), nine peaks

were clearly determined which were labeled A-I according to the chemical shift of their anomeric protons. The COSY, HSQC and HMBC experiments allowed partial assignment of the nine residues, and the result was shown in **Table 3**.

The intensive anomeric signals of **residue A** appeared at 5.15 ppm and 107.26 ppm, indicating a β-configuration of Gal*f* unit that had a relative high content in the galactomannan. The proton assignment of residue A (From H-2 to H-6/6': 4.08, 3.99, 4.00, 3.90 and 3.81/3.56 ppm) was obtained from COSY spectrum (**Fig. 2c**). The corresponding chemical shifts of carbon were 81.52, 76.96, 83.16, 69.89 and 69.52 ppm for C-2, C-3, C-4, C-5 and C-6, respectively, as revealed by HSQC spectrum (**Fig. 2d**). The downfield shift of C-6 led to the identification of residue A as β-1,6-Gal*f*. On the other hand, the **residue C**, which had H-1 and C-1 of 5.06 ppm and 106.13 ppm, was also endorsed as β-1,6-Gal*f* unit. The slight difference of chemical shifts for the 6-O substituted β-Gal*f* residues indicated the location of different chemical environments. The assignment of these two residues was also confirmed by comparing with the value from literatures (Bernabé, Salvachúa, Jiménez-Barbero, Leal, & Prieto, 2011; Bi, et al., 2013; Górska-Frączek, et al., 2011; Prieto, et al., 1997).

A complete assignment of signals derived from **residue F** and **G** was successfully achieved, as shown in **Fig. 2c** and **Table 3**. The β-configuration form of both residues was established by chemical shifts at 4.96 ppm (**residue F**) and 4.94 ppm (**residue G**) of H-1, as well as 108.12 ppm of C-1. The obvious downfield shift of C-5 of residue G (**Fig. 2d**), in addition to result from methylation analysis, allowed assigning residue G to β-1,5-Gal*f*. The residue F, on the other hand, without any ^{13}C shifts induced by glycosylation, was deduced to β-T-Gal*f*. Besides, both of the residues possessed all typical chemical shifts in comparison of the observed values with those reported in the literatures (Ahrazem, Leal, Prieto, Jiménez-Barbero, & Bernabé, 2001; Bernabé, et al., 2011; Giménez-Abián, Bernabé, Leal, Jiménez-Barbero, & Prieto, 2007; J. Leal, Jiménez-Barbero, Bernabé, & Prieto, 2008).

The anomeric chemical shift for **residue D** was 4.99/98.38 ppm, suggesting that it was an α-linked unit. The chemical shifts for the H2-6/6' of residue D were identified as 3.53, 3.64, 3.44, 3.62 and 3.82/3.72, respectively, by the well-resolved cross-peaks in the COSY spectrum, and the corresponding ^{13}C signals were identified from the HSQC spectrum. Comparing the chemical shifts

with the previous studies (Chen, Zhang, Chen, & Cheung, 2014; Guo, et al., 2012), for both protons and carbons, allowed to deduce residue D as α-T-Glc*p*.

However, the information for the other residues was poor due to overlapping of signals, both for ^{1}H and ^{13}C spectra, especially for the residue B, E and H. The anomeric signal of **residue B, E and H** was 5.15/101.24, 4.96/97.35 and 5.07/100.84 ppm, respectively. Through COSY spectrum (**Fig. 2c**), the chemical shift of H-2 was determined at 4.04, 4.04 and 4.08 ppm for residue B, E and H, respectively. Therefore, the corresponding C-2 chemical shift was figured out at 76.96, 76.96 and 76.61 ppm, respectively, by HSQC spectrum. The downfield shift of C-2s suggested that all the three residues carried a 2-O-subsituted carbon. Besides, the result from methylation analysis had evidenced the presence of 1,2-Man*p*, 1,2,6-Man*p* and 1,2,4,6-Man*p*. By comparison of the chemical shifts with those of previous reports (Omarsdottir, et al., 2006) and consideration of the methylation result, the residue B, E and H was deduced to α-1,2-Man*p*, α-1,2,6-Man*p* and α-1,2,4,6-Man*p*, respectively. With regard to residue I, the weak coupling between H-1 and H-2 precluded the discrimination and assignation of cross peaks. This assignment, however, was partially achieved in the current study by comparing the chemical shifts with literatures figures (Bernabé, et al., 2011; Jiménez-Barbero, Prieto, Gómez-Miranda, Leal, & Bernabé, 1995) and analyzing the cross peaks in the HSQC spectrum, thus contributing to identify **residue I** as α-1,6-Man*p*.

A long-range HMBC spectroscopy was employed to identify the sequences between glycosyl residues, as shown in **Fig. 2e** and summarized in **Table 3**. Cross-peaks of both anomeric protons and carbons of each glycosyl residue were examined. Cross-peaks were found between H-1 (5.15 ppm) of residue A and C-5 (75.91 ppm) of residue G (**A H-1, G C-5**); C-1 (107.26 ppm) of residue A and H-5 (3.89 ppm) of residue G (**A C-1, G H-5**). Similarly, cross-peaks between H-1 (4.96 ppm) of residue F and C-6 (69.52 ppm) of residue A (**F H-1, A C-6**); cross-peaks between H-1 (4.94 ppm) of residue G and C-6 (69.52 ppm) of residue A (**G H-1, A C-6)**; C-1 (108.12 ppm) of residue F/G and H-6/6' (3.56, 3.81 ppm) of residue A (**F/G C-1, A H-6/6'**) were observed. Cross-peaks between H-1 (4.94 ppm) of residue G and C-2 (76.69 ppm) of residue B/E (**G H-1, B/E C-2**), as well as C-1 (108.13 ppm) of residue G and H-2 (4.04 ppm) of residue B/E (**G C-1, B/E H-2**) were found. Likewise, weak cross-peaks between H-1 (5.06 ppm) of residue C and C-2 (76.96 ppm) of residue B/E (**C H-1, B/E C-2**); C-1 (106.13 ppm) of residue C and H-2 (4.04 ppm) of residue B/E

(**C C-1, B/E H-2**) were observed. Combining the above result, the following possible fragments of sequences in the galactomannan would be concluded:

β-D-Gal*f* (1→6)-β-D-Gal*f* (1→5)-β-D-Gal*f* (1→$_n$2)-α-D-Man*p* (1→
6
F **A** **G** **B/E**

β-D-Gal*f* (1→6)-β-D-Gal*f* (1→2)-α-D-Man*p* (1→
6
F **C** **B/E**

However, the correlations of the other sugar residues, especially those among residues B, E, H and I, were not unambiguous detected due to their low resonance signal intensity. As a result, not much information could be drawn through the current NMR experiments for the mannan core. Therefore, the NMR analysis for the hydrolysate (2h-I) was conducted to get the information of the mannopyranoses.

3.5 NMR spectroscopy analysis of the hydrolysate (2h-I)

In order to investigate the additional connections among these residues, a mild acid hydrolysis experiment was carried out to selectively hydrolyze the polysaccharide, taking the advantage of the lability of the glycosidic linkages of the furanoid rings, compared with that of the mannan pyranoid rings. Treatment with 0.1 TFA for 2 h at 100 ˚C removed the majority of the Gal*f* moiety as supported by the monosaccharide composition and methylation results. Therefore, 1D and 2D NMR spectra were further conducted for the hydrolysate (2h-I) to provide more detailed structural information of the main chain. The peaks in the anomeric region were designated **J** (4.82/99.31 ppm), **K** (5.16/100.67 ppm), **L** (5.14/100.61 ppm), **M** (5.03/98.16 ppm), **N** (4.96/102.22 ppm) and **O** (5.04/105.78 ppm), as marked in **Fig. 3a and 3b**. The ^{1}H and ^{13}C signals were assigned using COSY, TOCSY, HSQC, HMBC and NOESY spectrum, which were listed in **Table 4**.

Residue J showed the dominant intensity both in the ^{1}H and ^{13}C spectrum, and was tentatively assigned to α-1,6-Man*p*. The chemical shifts of H-1, H-2, H-3, H-4, H-5 and H6/6’ were successfully obtained from the COSY spectrum (**Fig. 3c**), which was 4.82, 3.91, 3.75, 3.65, 3.78 and 3.71/3.86, respectively. Additionally, following the dotted **J** line marked in the TOCSY spectrum (**Fig. 3d**), five signals at 3.91, 3.86, 3.78, 3.75 and 3.65 ppm were clearly observed, matched well with the chemical shifts from COSY spectrum, except for the signals of 3.71 ppm due

307 to the overlapping. The chemical shifts for C-1 to C-6 of this residue were demonstrated to be 99.31,
308 69.91, 70.67, 66.53, 70.64 and 65.43 ppm based on the cross-peaks in the HSQC spectrum (**Fig. 3e**).
309 The assignment was in accordance with the values reported by the literature (Bernabé, et al., 2011;
310 Bi, et al., 2011; Jiménez-Barbero, et al., 1995).
311 In the HSQC spectrum, the anomeric proton signals at δ 5.16 ppm (**residue K**) and 5.14 ppm
312 (**residue L**) that correlated with the anomeric carbon signal at δ 100.67 ppm and δ 100.61 ppm,
313 respectively, were both endorsed as α-1,2-Man*p*. According to COSY spectrum, the H-2, H-3 and
314 H-4 were determined at 4.03, 3.88 and 3.69 ppm for residue K, and 4.02, 3.87 and 3.66 ppm for
315 residue L, respectively. Due to the severe crowding and low intensity of the cross peaks, it was
316 difficult to achieve an unambiguous assignment of all the signals. This issue, however, was
317 addressed by examining the cross peaks through TOCSY and HSQC spectrum (**Fig. 3d and 3e**),
318 together with comparing the data from the previous reports (Molinaro, Piscopo, Lanzetta, & Parrilli,
319 2002; Omarsdottir, et al., 2006). The full assignment of ^{1}H and ^{13}C was also obtained and was
320 summarized in **Table 4**.
321 The cross peak at 5.03/98.16 ppm in the anomeric region of HSQC spectrum was tentatively
322 assigned to α-1,2,6-Man*p* (**residue M**). The chemical shifts of H-2 (3.95 ppm), H-3 (3.89 ppm) and
323 H-4 (3.61 ppm) was achieved by the well-resolved cross peaks in the COSY spectrum (**Fig. 3c**), and
324 was also confirmed in the TOCSY spectrum (**Fig. 3d,** Line M). But the chemical shifts of H-5 and
325 H-6/6' were unobtainable because of the relative low abundance and high degree of signal
326 overlapping due to the structural similarity. The assignment of some peaks was derived from HSQC
327 spectroscopy, and meantime the corresponding chemical shifts of carbon were also identified from
328 that spectrum, as listed in **Table 4**.
329 The chemical shift of ^{1}H at 4.96 ppm and ^{13}C at 102.22 ppm indicated that **residue N** should be
330 assigned to α-T-Man*p*. The chemical shifts for the H-1, H-2, H-3, H-4, H-5 and H-6/6' were
331 identified as 4.96, 3.99, 3.76, 3.57, 3.68 and 3.68/3.80 ppm, respectively, through COSY spectrum.
332 The corresponding chemical shifts for C-1 to C-6 were achieved in HSQC spectrum, and the result
333 was in consistence with the literature values (Molinaro, et al., 2002; Omarsdottir, et al., 2006), which
334 confirmed the assignment of residue N.
335 Examining the cross-peaks of both the anomeric proton and carbon in the HMBC spectrum, the

sequence of glycosyl residues of this polysaccharide was evidenced (**Fig. 3f**). Obviously, residue J correlated with two sugar residues both at C-6 and H-6, residue J (**J H-1, J C-6; J C-1, J H-6/6'**) and residue M **(J H-1, M C-6; J C-1, M H-6/6'**). Besides, cross-peaks between H-1 (5.03 ppm) of residue M and C-6 (65.43 ppm) of residue J (**M H-1, J C-6**); C-1 (98.16 ppm) of residue M and H-6 (3.86 ppm) of residue J (**M C-1, J H-6**) was also found. Thus, the following sequences were established:

→6)-α-D-Man*p* (1→6)-α-D-Man*p* (1→ →6)-α-D-Man*p* (1→6)-α-D-Man*p* (1→
J **J** ↑2
J **M**

In addition, cross-peaks between the H-1 (5.16 ppm) of residue K and C-2 (78.63 ppm) of residue M (**K H-1, M C-2**); C-1 (100.67 ppm) of residue K and H-2 (3.95 ppm) of residue M (**K C-1, M H-2**); H-1 (5.14 ppm) of residue L and C-2 (78.09 ppm) of residue L (**L H-1, L C-2**); C-1 (100.61 ppm) of residue L and H-2 (4.02 ppm) of residue L (**L C-1, L H-2**) was observed. Besides, cross-peak between H-1 (5.04 ppm) of residue O and C-2 (78.63 ppm) of residue M (**O H-1, M C-2**) was also clearly evidenced. And this cross-peak suggested that the remaining small percentage of β-D-Gal*f* was directly linked to the backbone at O-2 of α-1,2,6-Man*p*. The following sequences were therefore indicated:

→2)-α-D-Man*p* (1→2)-α-D-Man*p* (1→ →2)-α-D-Man*p* (1→2)-α-D-Man*p* (1→
↑6 **L** **L**
K **M**

β-D-Gal*f* (1→2)-α-D-Man*p* (1→
↑6
O **M**

With regard to residue N, the H-1 (4.96 ppm) correlated with C-2 (78.09 ppm) of residue K/L (**N H-1, K/L C-2**) and C-2 (78.63 ppm) of residue M (**N H-1, M C-2**), and the C-1 (102.22 ppm) showed obviously cross-peak with H-2 (4.03 ppm) of residue K (**N C-1, K H-2**) and H-2 (4.02 ppm) of residue L (**N C-1, L H-2**), suggesting the presence of the following sequences:

α-D-Man*p* (1→2)-α-D-Man*p* (1→ α-D-Man*p* (1→2)-α-D-Man*p* (1→
↑6 **N** **K/L**
N **M**

NOESY spectroscopy correlates nuclei through space, so both the inter- and intra-residual connectivities could be observed, which not only confirmed the assignments of chemical shifts for

the illustrated sugar residues, but demonstrated the aforementioned sequences of glycosidic linkages, as shown in **Fig. 3g**.

Although the linkage information of α-1,2,4,6-Man*p* residue was not sufficient enough from the above NMR spectrums due to its relative low content and structural similarity, the methylation result together with monosaccharide composition deduced its presence in the main chain. A significant decrease of the content was observed after treating with mild acid, suggesting the branches that linked to α-1,2,4,6-Man*p* were probably Gal*f* chains.

Combined all the data from the galactomannan and its hydrolysate (2h-I), the idealized structure of the polysaccharide was proposed to be:

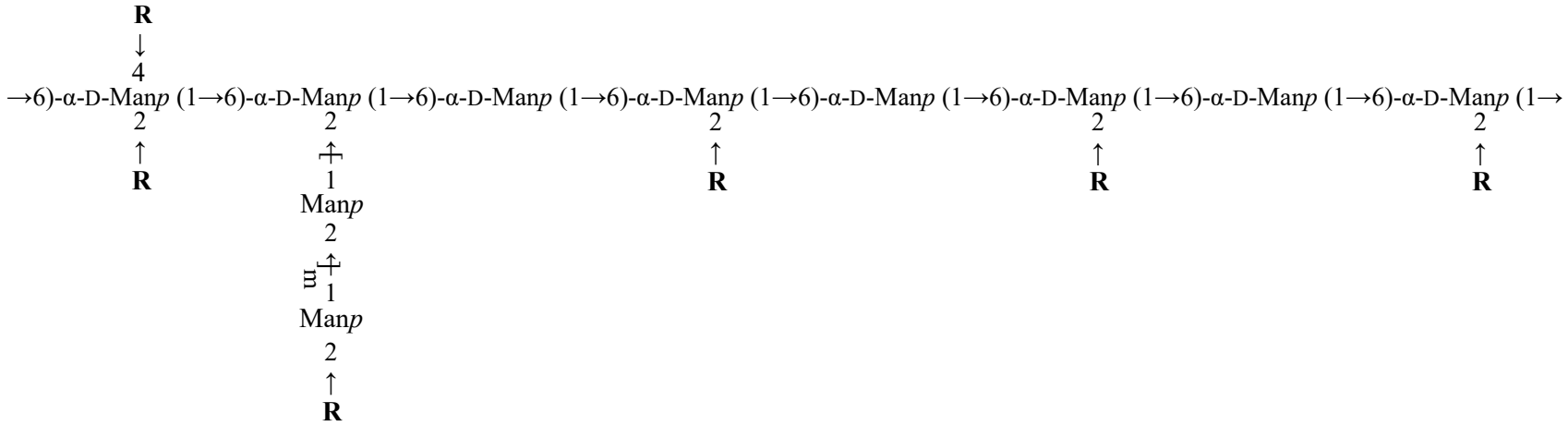

m might be 0, 1 or 2.

R could be as follows:

β-D-Gal*f* (1→6)-β-D-Gal*f* (1→5)-β-D-Gal*f* (1→$_{n}$ (major), **n** might be 1 or 2; β-D-Gal*f* (1→6)-β-D-Gal*f* (1→ (minor);

4. Conclusion

In the present study, a novel α-1,6-linked galactomannan was obtained from water-insoluble residues of natural *C. sinensis* through alkali extraction. The Mw and intrinsic viscosity of this galactomannan was 7207 and 0.032 dL/g, respectively, and it was composed of galactose, glucose and mannose in a percentage of 68.65%, 6.65% and 24.02%, with trace amount of rhamnose. The backbone of this galactomannan was made up of linear α-1,6-Man*p*. The major branches, composed of β-1,6-Gal*f* and β-1,5-Gal*f*, were linked to *O*-2 and *O*-4 of the backbone. Another kind of branch was composed of β-1,6-Gal*f* and β-1,5-Gal*f* linking to the C-2 of α-1,2-Man*p* residues attaching to the main chain. All the branches were terminated at β-T-Gal*f*. The possible structure of this novel galactomannan was established. This study provided substantial updated structural information for the polysaccharide from *C. sinensis*.

Acknowledgments

The financial support from the National Natural Science Foundation of China for Excellent Young Scholars (31422042), the Key Project of International Cooperation of Jiangxi Provincial Department of Science and Technology (20141BDH80009), the Project of Science and Technology of Jiangxi Provincial Education Department (KJLD13004) and Research Project of State Key Laboratory of Food Science and Technology (SKLF-ZZB-201508, SKLF-ZZA-201611) is gratefully acknowledged.

The authors would like to thank Mrs. Yajing Li of Qinghai Ta Er Sheng Gu Agricultural Science and Technology Co. Ltd. Company, for providing the samples of natural *C. sinensis*. In addition, the authors wish to thank Prof. Qi Wang, Ms. Cathy Wang and Dr. Qingbin Guo of Agriculture and Agri-Food Canada for technical assistance and insightful discussion.

References

Ahrazem, O., Leal, J., Prieto, A., Jiménez-Barbero, J., & Bernabé, M. (2001). Chemical structure of a polysaccharide isolated from the cell wall of *Arachniotus verruculosus* and *A. ruber*. *Carbohydrate Research, 336*(4), 325-328.

Bernabé, M., Salvachúa, D., Jiménez-Barbero, J., Leal, J. A., & Prieto, A. (2011). Structures of wall heterogalactomannans isolated from three genera of entomopathogenic fungi. *Fungal Biology, 115*(9), 862-870.

Bi, H., Gao, T., Li, Z., Ji, L., Yang, W., Iteku, B. J., et al. (2013). Structural elucidation and antioxidant

activity of a water-soluble polysaccharide from the fruit bodies of *Bulgaria inquinans* (Fries). *Food Chemistry, 138*(2), 1470-1475.

Bi, H., Han, H., Li, Z., Ni, W., Chen, Y., Zhu, J., et al. (2011). A water-soluble polysaccharide from the fruit bodies of *Bulgaria inquinans* (Fries) and its anti-malarial activity. *Evidence-Based Complementary and Alternative Medicine, 2011*.

Chen, L., Zhang, B.-B., Chen, J.-L., & Cheung, P. C. (2014). Cell wall structure of mushroom sclerotium (*Pleurotus tuber-regium*): Part 2. Fine structure of a novel alkali-soluble hyper-branched cell wall polysaccharide. *Food Hydrocolloids, 38*, 48-55.

Chen, P. X., Wang, S., Nie, S., & Marcone, M. (2013). Properties of *Cordyceps sinensis*: A review. *Journal of Functional Foods, 5*(2), 550-569.

Ciucanu, I., & Kerek, F. (1984). A simple and rapid method for the permethylation of carbohydrates. *Carbohydrate Research, 131*(2), 209-217.

Górska-Frączek, S., Sandström, C., Kenne, L., Rybka, J., Strus, M., Heczko, P., et al. (2011). Structural studies of the exopolysaccharide consisting of a nonasaccharide repeating unit isolated from *Lactobacillus rhamnosus* KL37B. *Carbohydrate Research, 346*(18), 2926-2932.

Giménez-Abián, M. I., Bernabé, M., Leal, J. A., Jiménez-Barbero, J., & Prieto, A. (2007). Structure of a galactomannan isolated from the cell wall of the fungus *Lineolata rhizophorae*. *Carbohydrate Research, 342*(17), 2599-2603.

Guo, Q., Cui, S. W., Kang, J., Ding, H., Wang, Q., & Wang, C. (2015). Non-starch polysaccharides from American ginseng: physicochemical investigation and structural characterization. *Food Hydrocolloids, 44*, 320-327.

Guo, Q., Cui, S. W., Wang, Q., Hu, X., Kang, J., & Yada, R. Y. (2012). Structural characterization of a low-molecular-weight heteropolysaccharide (glucomannan) isolated from *Artemisiasphaerocephala Krasch*. *Carbohydrate research, 350*, 31-39.

Jiménez-Barbero, J., Prieto, A., Gómez-Miranda, B., Leal, J. A., & Bernabé, M. (1995). Chemical structure of fungal cell-wall polysaccharides isolated from *Microsporum gypseum* and related species of *Microsporum* and *Trychophyton*. *Carbohydrate Research, 272*(1), 121-128.

Kiho, T., Tabata, H., Ukai, S., & Hara, C. (1986). A minor, protein-containing galactomannan from a sodium carbonate extract of *Cordyceps sinensis*. *Carbohydrate Research, 156*, 189-197.

Leal, J., Jiménez-Barbero, J., Bernabé, M., & Prieto, A. (2008). Structural elucidation of a cell wall fungal polysaccharide isolated from *Ustilaginoidea virens*, a pathogenic fungus of *Oriza sativa* and *Zea mays*. *Carbohydrate Research, 343*(17), 2980-2984.

Leal, J. A., Prieto, A., Bernabé, M., & Hawksworth, D. L. (2010). An assessment of fungal wall heteromannans as a phylogenetically informative character in ascomycetes. *FEMS Microbiology Reviews, 34*(6), 986-1014.

Miyazaki, T., Oikawa, N., & Yamada, H. (1977). Studies on fungal polysaccharides. XX. Galactomannan of *Cordyceps sinensis*. *Chemical and Pharmaceutical Bulletin, 25*(12), 3324-3328.

Molinaro, A., Piscopo, V., Lanzetta, R., & Parrilli, M. (2002). Structural determination of the complex exopolysaccharide from the virulent strain of *Cryphonectria parasitica*. *Carbohydrate Research, 337*(19), 1707-1713.

Nie, S.-P., Cui, S. W., Phillips, A. O., Xie, M.-Y., Phillips, G. O., Al-Assaf, S., et al. (2011). Elucidation of the structure of a bioactive hydrophilic polysaccharide from Cordyceps sinensis by methylation analysis and NMR spectroscopy. *Carbohydrate Polymers, 84*(3), 894-899.

Nie, S., Cui, S. W., Xie, M., Phillips, A. O., & Phillips, G. O. (2013). Bioactive polysaccharides from

Cordyceps sinensis: Isolation, structure features and bioactivities. *Bioactive Carbohydrates and Dietary Fibre, 1*(1), 38-52.

Omarsdottir, S., Petersen, B., Barsett, H., Paulsen, B. S., Duus, J., & Olafsdottir, E. (2006). Structural characterisation of a highly branched galactomannan from the lichen *Peltigera canina* by methylation analysis and NMR-spectroscopy. *Carbohydrate Polymers, 63*(1), 54-60.

Omarsdottir, S., Petersen, B. O., Paulsen, B. S., Togola, A., Duus, J. Ø., & Olafsdottir, E. S. (2006). Structural characterisation of novel lichen heteroglycans by NMR spectroscopy and methylation analysis. *Carbohydrate Research, 341*(14), 2449-2455.

Prieto, A., Leal, J. A., Poveda, A., Jiménez-Barbero, J., Gómez-Miranda, B., Domenech, J., et al. (1997). Structure of complex cell wall polysaccharides isolated from *Trichoderma* and *Hypocrea* species. *Carbohydrate Research, 304*(3), 281-291.

Qian, K.Y., Cui, S. W., Nikiforuk, J., & Goff, H. D. (2012). Structural elucidation of rhamnogalacturonans from flaxseed hulls. *Carbohydrate Research, 362*, 47-55.

Wang, J., Kan, L., Nie, S., Chen, H., Cui, S. W., Phillips, A. O., et al. (2015). A comparison of chemical composition, bioactive components and antioxidant activity of natural and cultured *Cordyceps sinensis*. *LWT-Food Science and Technology, 63*(1), 2-7.

Wang, J., Nie, S., Cui, S. W., Wang, Z., Phillips, A. O., Phillips, G. O., et al. (2017). Structural characterization and immunostimulatory activity of a glucan from natural Cordyceps sinensis. *Food Hydrocolloids*, *67*, 139-147.

Wang, J., Nie, S., Kan, L., Chen, H., Cui, S. W., Phillips, A. O., et al. (2017). Comparison of structural features and antioxidant activity of polysaccharides from natural and cultured *Cordyceps sinensis*. *Food Science and Biotechnology*, *26(1)*, 55-62.

Zhang, M., Cui, S., Cheung, P., & Wang, Q. (2007). Antitumor polysaccharides from mushrooms: a review on their isolation process, structural characteristics and antitumor activity. *Trends in Food Science & Technology, 18*(1), 4-19.

FIGURES

Figure 1

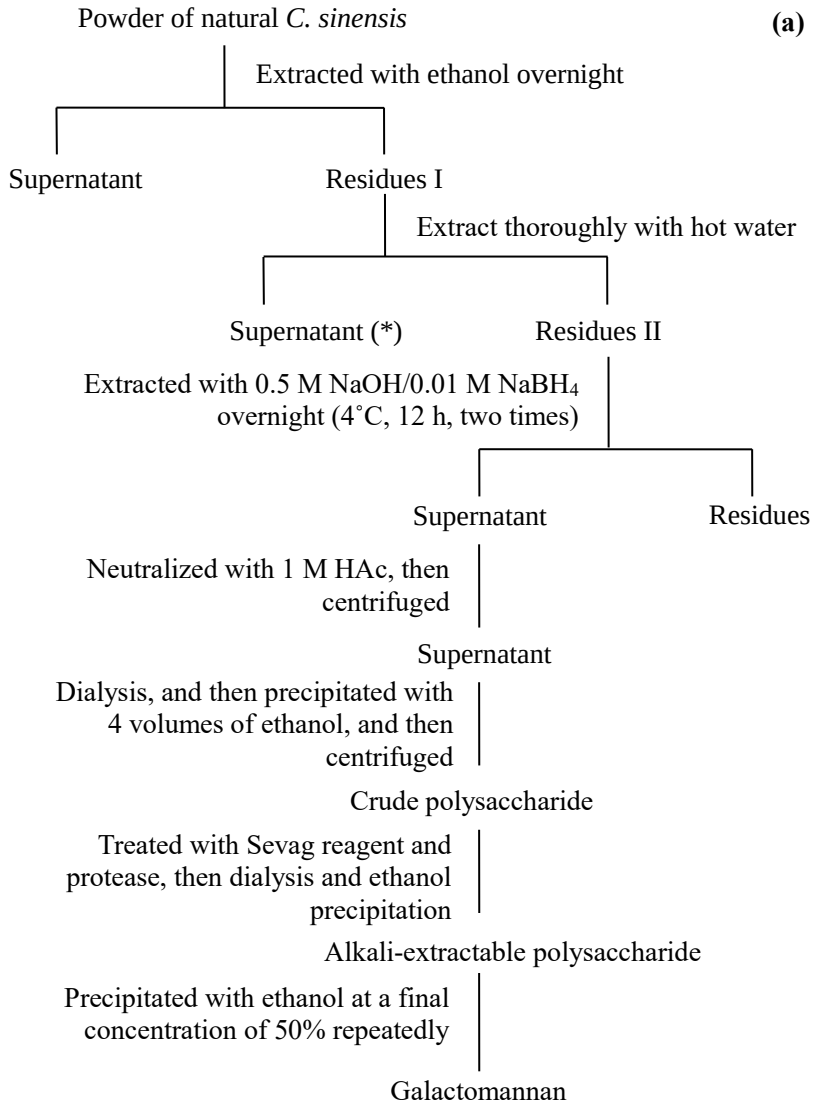

* This fraction was further isolated and purified to obtain the water-extracted polysaccharide, as described in our previous report (Wang, et al., submitted for publication)

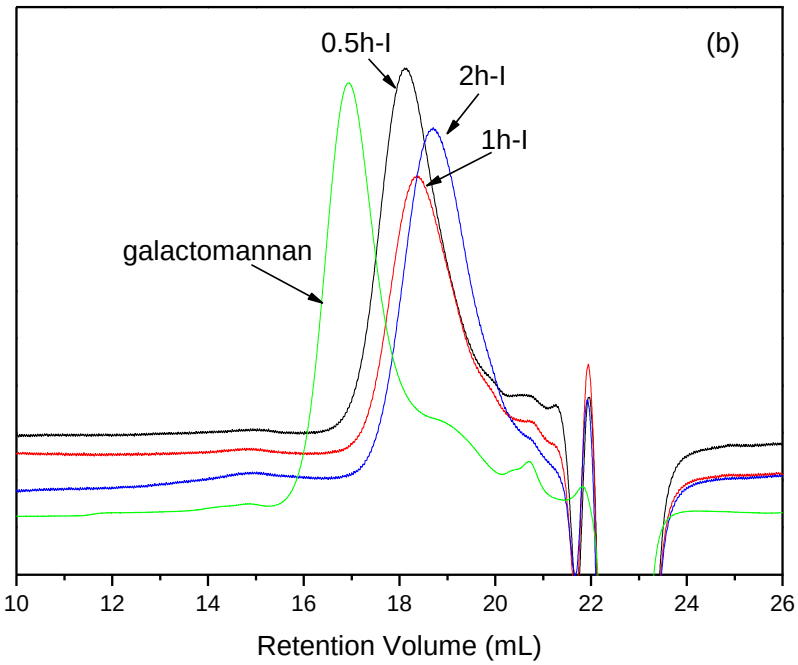
0.5h-I
2h-I
1h-I
(b)
galactomannan
10
12
14
16
18
20
22
24
26
Retention Volume (mL)

493

494

Figure 2

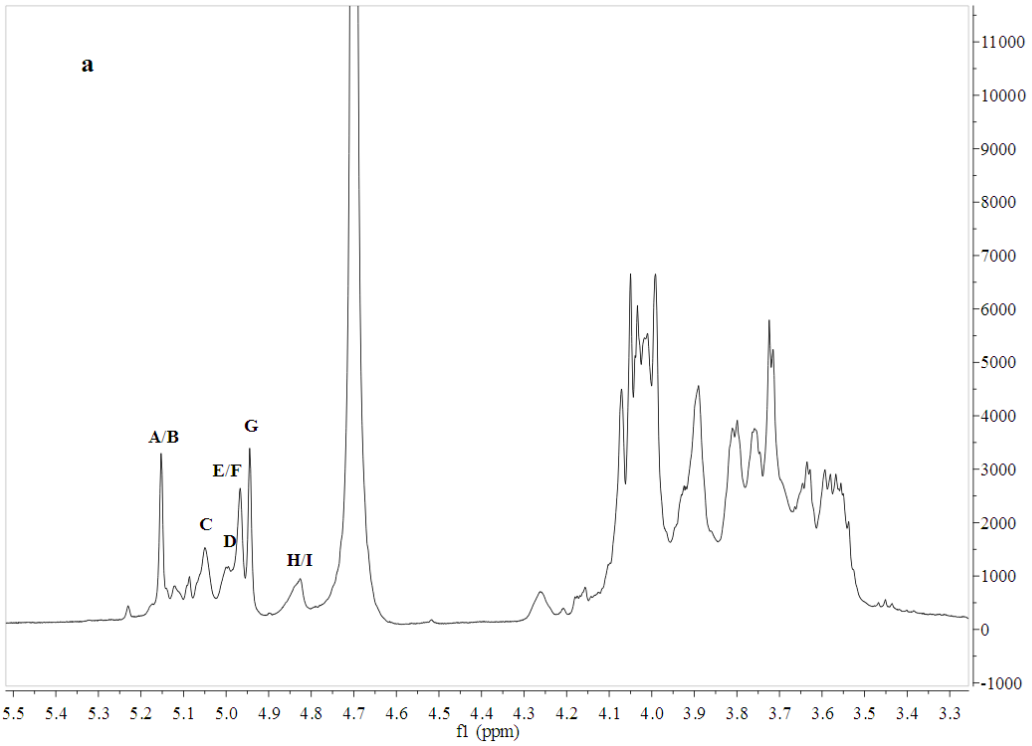
a
A/B
C
D
E/F
G
H/I
11000
10000
9000
8000
7000
6000
5000
4000
3000
2000
1000
0
-1000
5.5 5.4 5.3 5.2 5.1 5.0 4.9 4.8 4.7 4.6 4.5 4.4 4.3 4.2 4.1 4.0 3.9 3.8 3.7 3.6 3.5 3.4 3.3
f1 (ppm)

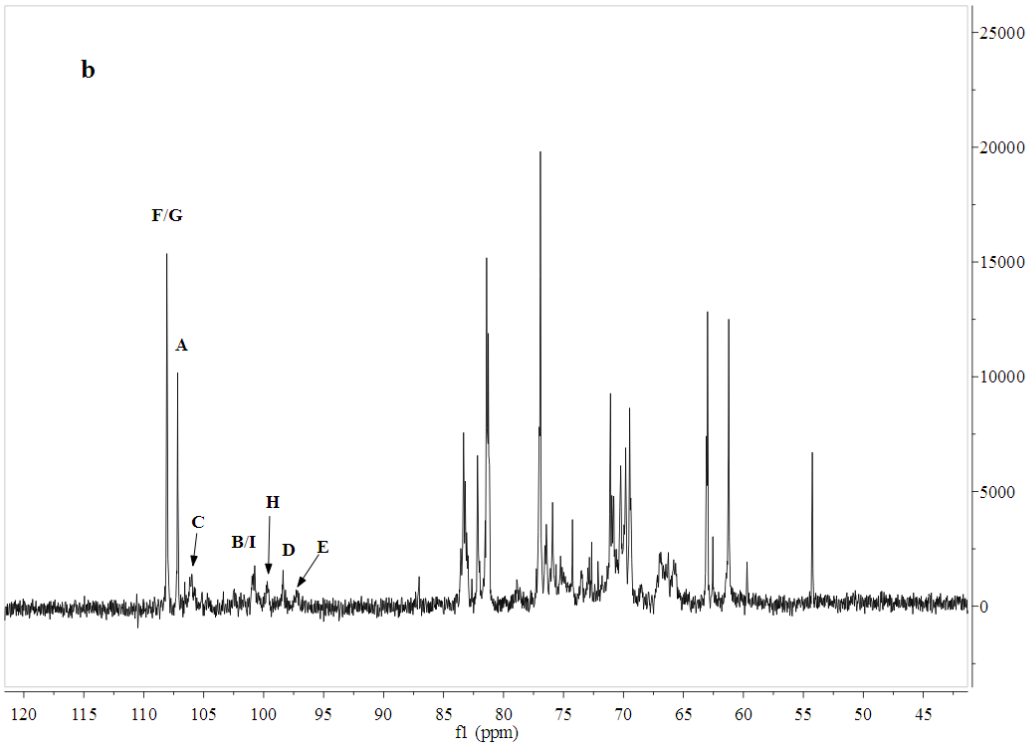
b
F/G
A
C
B/I
H
D
E
25000
20000
15000
10000
5000
0
120 115 110 105 100 95 90 85 80 75 70 65 60 55 50 45
f1 (ppm)

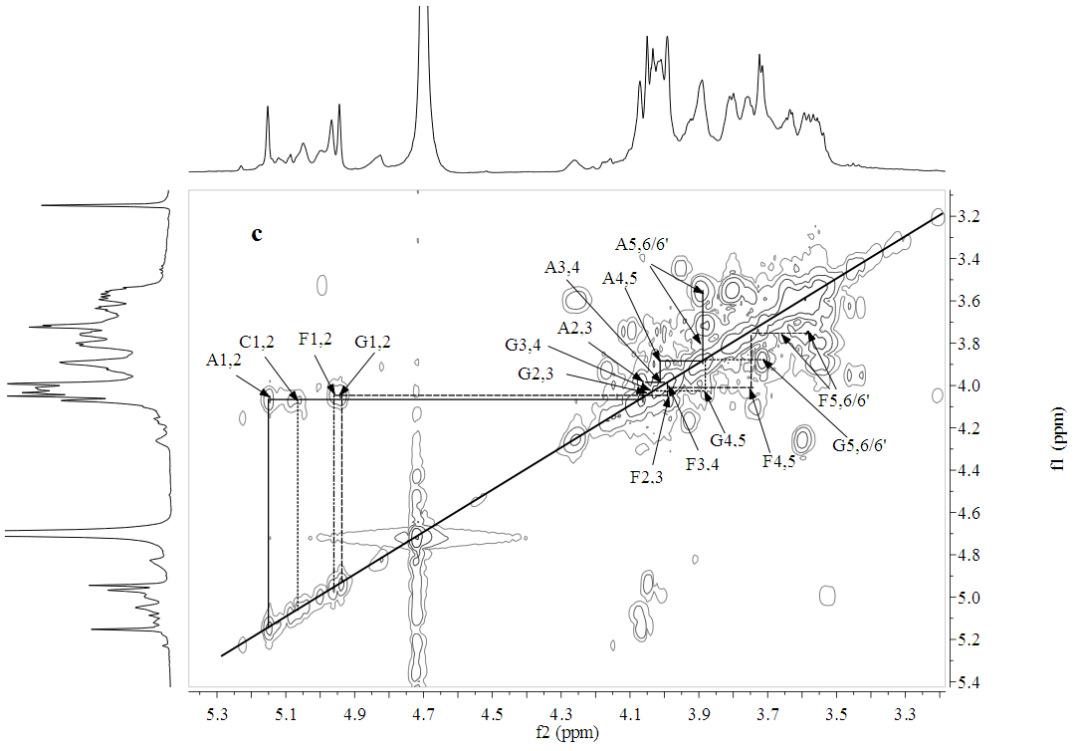
c
A1,2
C1,2
F1,2
G1,2
A3,4
A4,5
A5,6/6'
A2,3
G3,4
G2,3
F5,6/6'
G4,5
F4,5
G5,6/6'
F2,3
F3,4
f2 (ppm)
f1 (ppm)

498

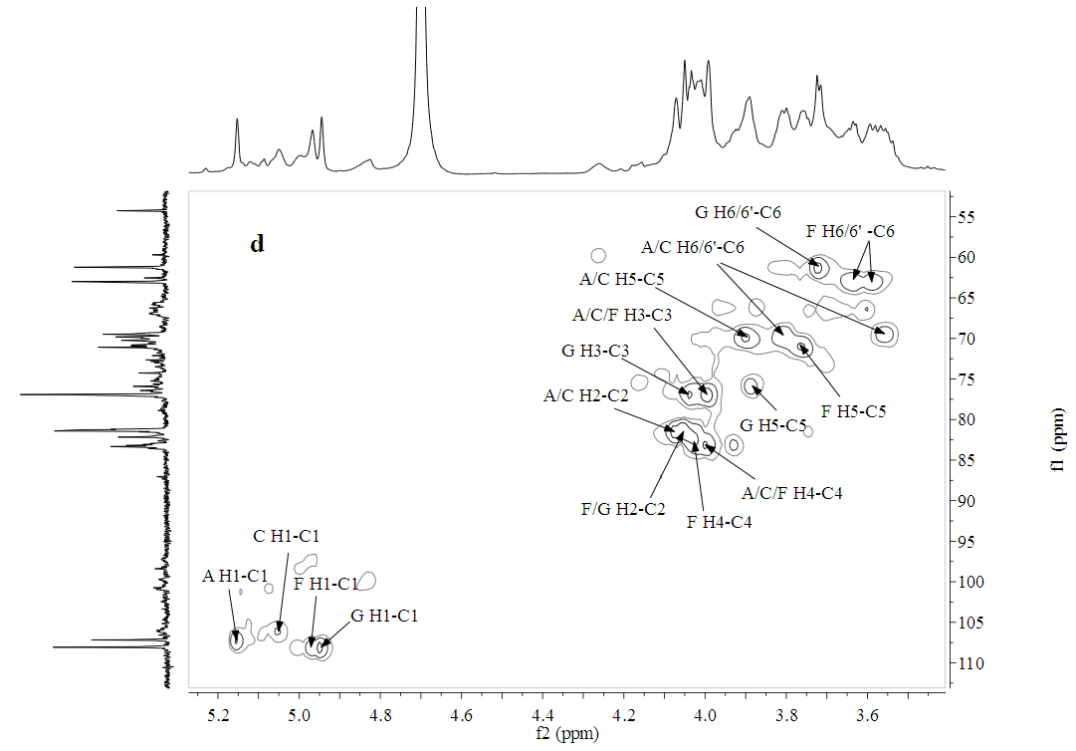
d
G H6/6'-C6
F H6/6' -C6
A/C H6/6'-C6
A/C H5-C5
A/C/F H3-C3
G H3-C3
A/C H2-C2
F H5-C5
G H5-C5
A/C/F H4-C4
F/G H2-C2
F H4-C4
C H1-C1
A H1-C1
F H1-C1
G H1-C1
f2 (ppm)
f1 (ppm)

499

500

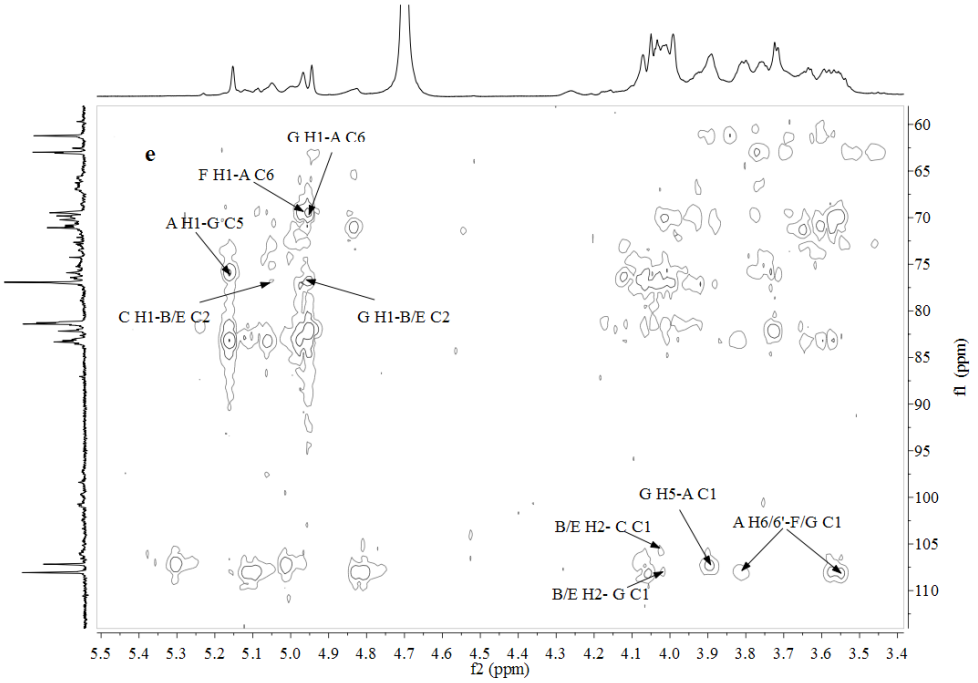

501

502

503

504

505 **Figure 3**

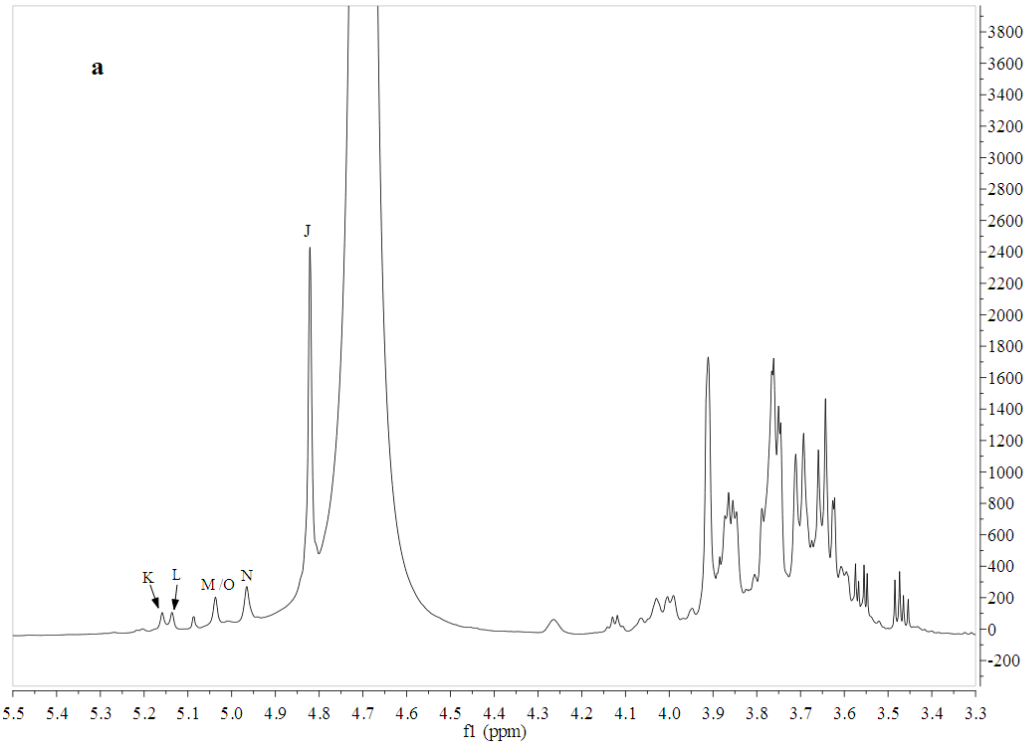

506

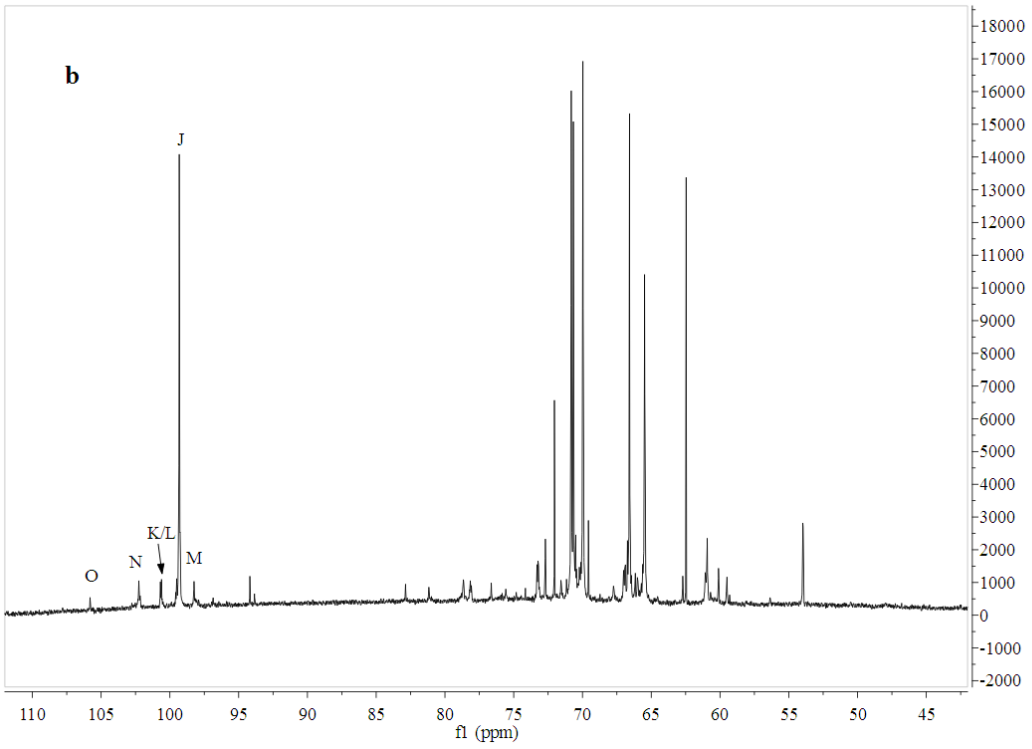

507

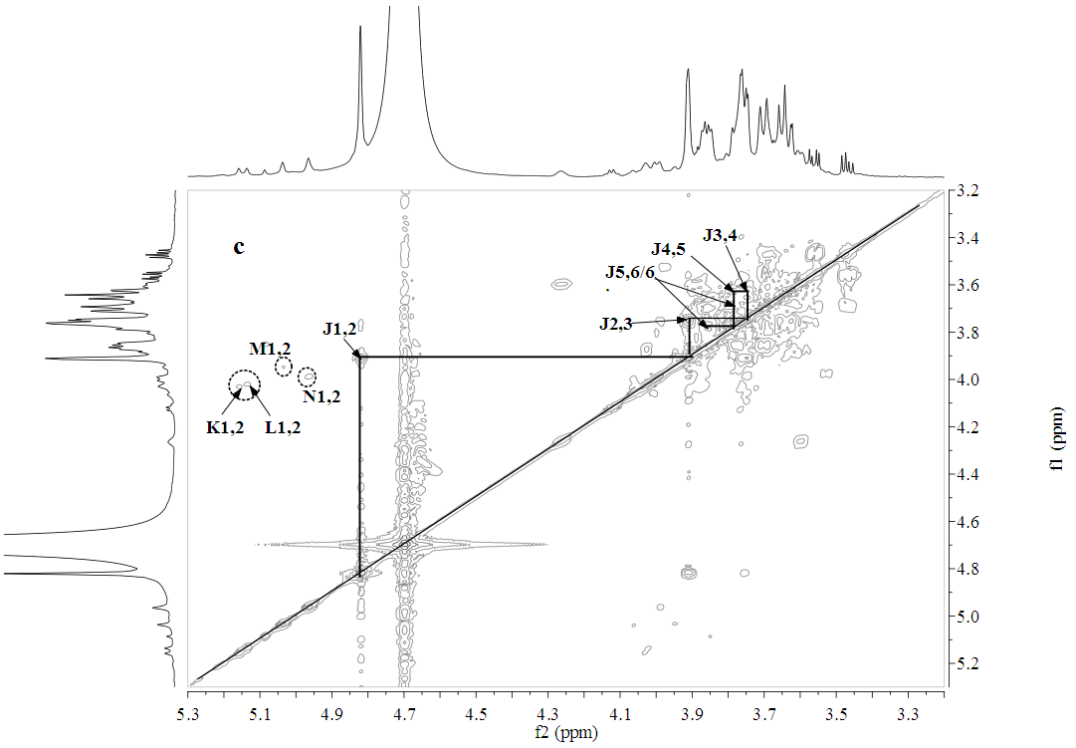
c
J1,2
J2,3
J3,4
J4,5
J5,6/6
M1,2
N1,2
K1,2
L1,2
f2 (ppm)
f1 (ppm)

508

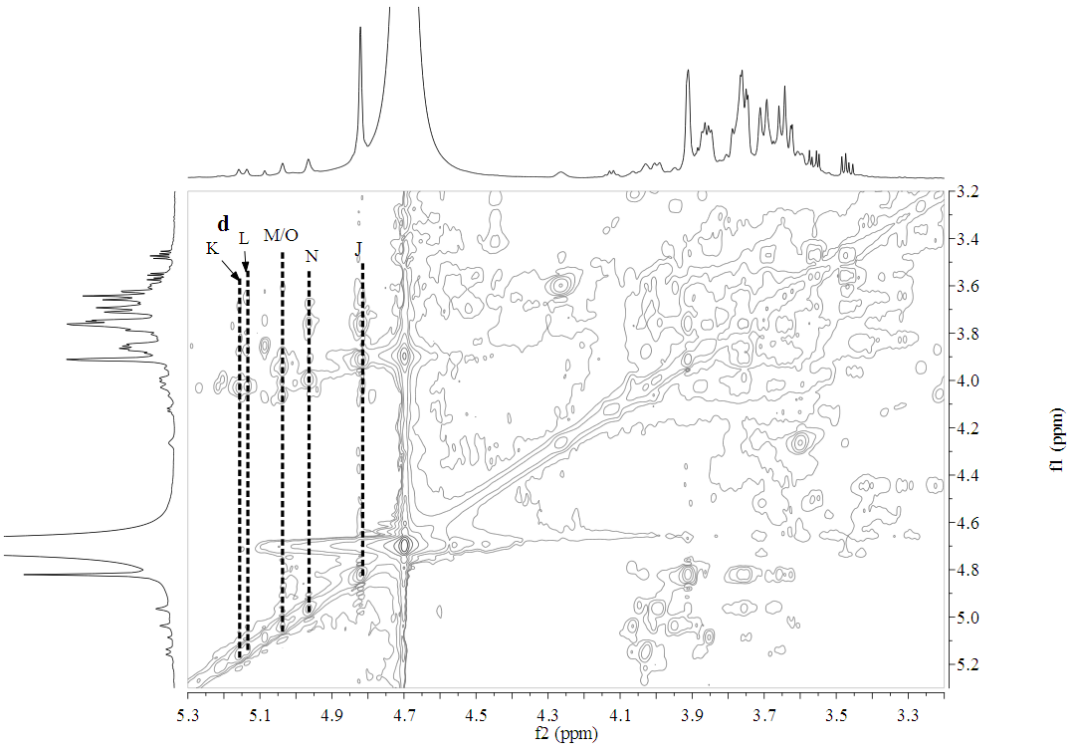
d
K
L
M/O
N
J
f2 (ppm)
f1 (ppm)

509

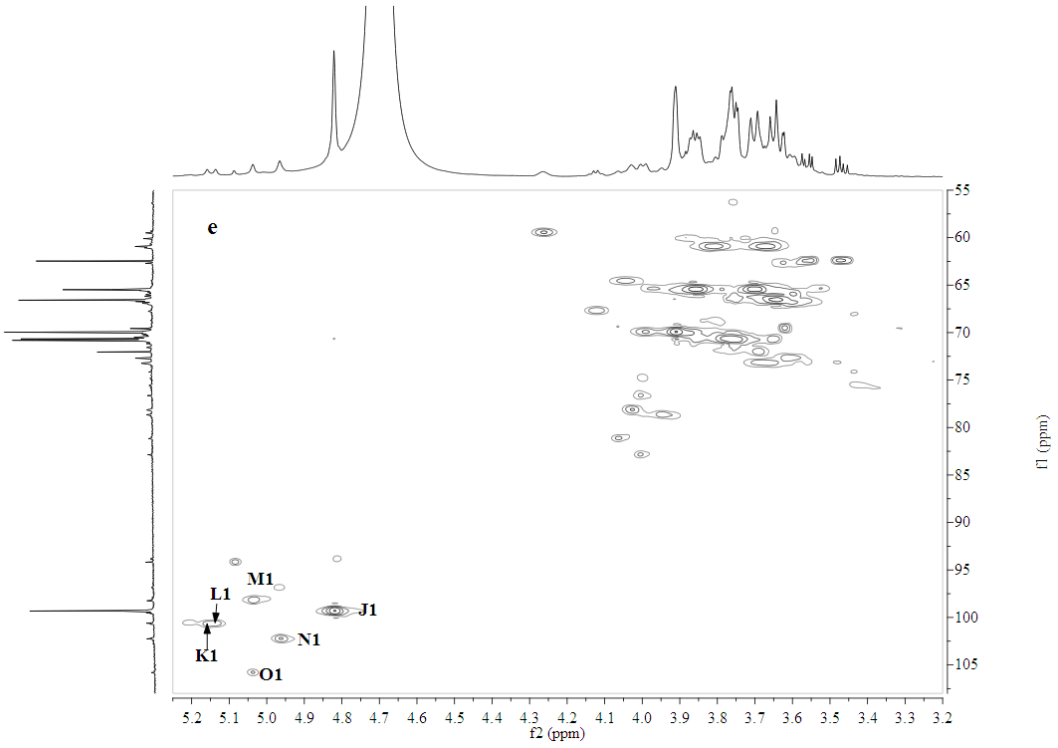
e
M1
L1
J1
N1
K1
O1
f2 (ppm)
f1 (ppm)

510

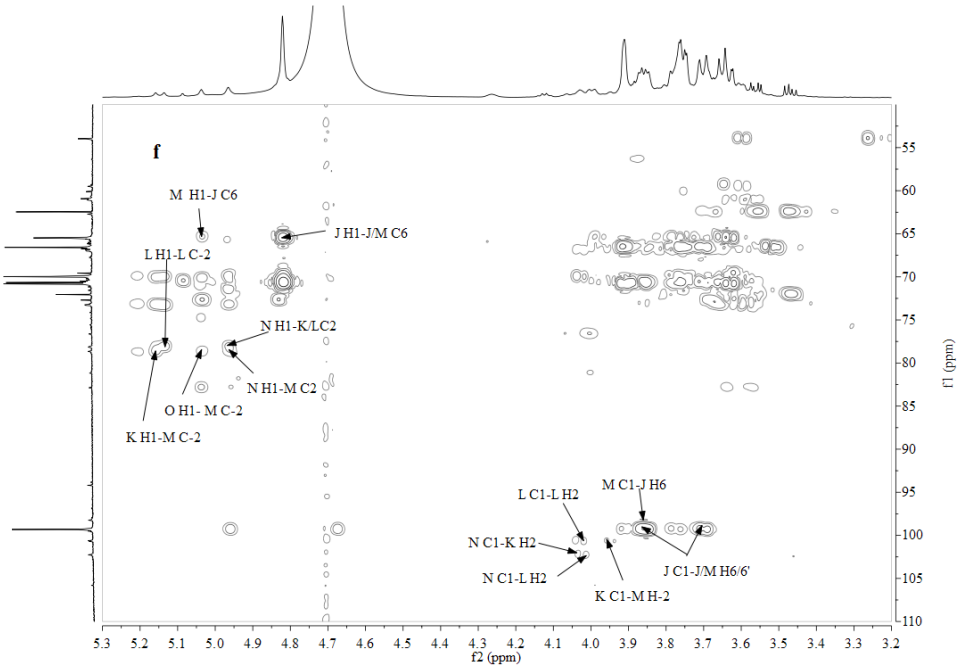
f
M H1-J C6
J H1-J/M C6
L H1-L C-2
N H1-K/LC2
N H1-M C2
O H1- M C-2
K H1-M C-2
L C1-L H2
M C1-J H6
N C1-K H2
N C1-L H2
J C1-J/M H6/6'
K C1-M H-2
f2 (ppm)
f1 (ppm)

511

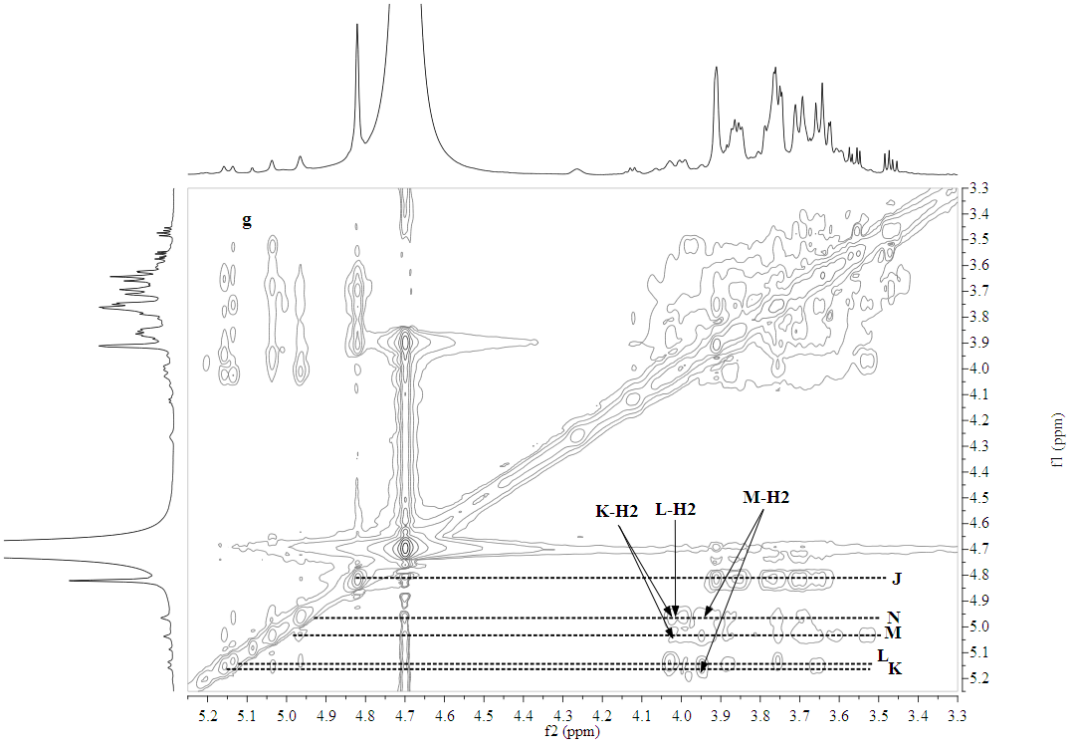

512

513

514

515

516

TABLES

Table 1 Monosaccharide composition of the galactomannan and its hydrolysates after partial acid hydrolysis

	Proportion (%)						
		Inside of dialysis bag			Outside of dialysis bag		
Monosaccharide	galactomannan	0.5 h	1 h	2 h	0.5 h	1 h	2 h
Rha	0.67	1.37	nd	nd	nd	nd	nd
Gal	68.65	22.17	2.77	3.96	97.57	94.65	90.62
Glc	6.65	5.80	7.57	13.82	2.43	1.78	2.79
Man	24.02	70.66	89.66	82.22	nd	3.57	6.59

nd not detected.

Table 2 GC-MS of alditol acetate derivatives from the methylated products of the galactomannan and its hydrolysate (2h-I)

Retention time	Permethylated alditol acetate	Mol (%) [a] galactomannan	Mol (%) [a] hydrolysate (2h-I)	Deduced Linkage type
28.44	2,3,4,6-Me_4 Glc and Man	5.03	15.59	T-Glc*p*/Man*p*
28.69	2,3,5,6-Me_4 Gal	16.72	3.33	T-Gal*f*
29.26	2,3,4,6-Me_4 Gal	0.78	1.88	T-Gal*p*
31.85	3,4,6-Me_3 Man	6.72	7.37	1,2-Man*p*
31.98	2,4,6-Me_3 Glc	nd	3.38	1,3-Glc*p*
32.06	2,3,6-Me_3 Gal	18.54	0.79	1,5-Gal*f*
32.32	2,3,6- Me_3 Glc	1.87	0.89	1,4-Glc*p*
32.38	2,4,6-Me_3 Gal	nd	0.71	1,3-Gal*p*
33.03	2,3,4-Me_3 Man	11.03	51.98	1,6-Man*p*
33.76	2,3,5-Me_3 Gal	10.55	0.36	1,6-Gal*f*
34.53	4,6-Me_2 Glc	1.47	0.68	1,2,3-Glc*p*
35.05	3,6-Me_2 Man	0.62	nd	1,2,4-Man*p*
35.81	2,3-Me_2 Man	4.76	2.95	1,4,6-Man*p*
36.27	3,4-Me_2 Man	15.56	7.25	1,2,6-Man*p*
36.73	2,4-Me_2 Man	1.21	2.13	1,3,6-Glc*p*
37.25	3,6-Me_2 Gal or Glc	0.99	nd	1,2,4-Gal*p*/Glc*p*
39.39	3-Me Man	4.17	0.70	1,2,4,6-Man*p*

nd: not detected.

[a] molar ratio of each sugar residue is based on the percentage of its peak area.

Table 3 ^{1}H and ^{13}C NMR chemical shifts of the galactomannan (2h-I) in D_2O at 294 K.

	Residues	H1/C1	H2/C2	H3/C3	H4/C4	H5/C5	H6/C6	H6’
A	β-1,6-Gal*f*	5.15	4.08	3.99	4.00	3.90	3.81	3.56
		107.26	81.52	76.96	83.16	69.89	69.52	
B	α-1,2-Man*p*	5.15	4.04	3.90	-[a]	-	-	-
		101.24	76.96	69.87	-	-	-	
C	β-1,6-Gal*f*	5.06	4.08	3.99	4.00	3.90	3.81	3.56
		106.13	81.52	76.96	83.16	69.89	69.52	
D	α-T-Glc*p*	4.99	3.53	3.64	3.44	3.62	3.82	3.72
		98.38	71.33	72.93	72.35	73.04	61.30	
E	α-1,2,6-Man*p*	4.96	4.04	-	-	-	-	-
		97.35	76.96	-	-	-	-	
F	β-T-Gal*f*	4.96	4.05	3.99	4.00	3.75	3.64	3.59
		108.12	81.44	76.96	83.16	70.99	63.05	
G	β-1,5-Gal*f*	4.94	4.05	4.04	4.03	3.89	3.72	3.72
		108.12	81.44	76.96	83.14	75.91	61.30	
H	α-1,2,4,6-Man*p*	5.07	4.08	-	-	-	-	-
		100.84	76.61	-	-	-	-	
I	α-1,6-Man*p*	4.83	3.91	3.75	3.63	-	3.88	3.69
		99.84	69.89	70.99	66.69	-	66.34	

[a] not obtained due to low resolution.

534 **Table 4 The ^{1}H and ^{13}C NMR chemical shifts of the hydrolysate (2h-I) in D_2O at 313K**

	Residues	H1/C1	H2/C2	H3/C3	H4/C4	H5/C5	H6/C6	H6’
J	α-1,6-Man*p*	4.82	3.91	3.75	3.65	3.78	3.70	3.86
		99.31	69.91	70.67	66.53	70.64	65.43	
K	α-1,2-Man*p* [a]	5.16	4.03	3.88	3.69	3.81	3.67	3.81
		100.67	78.09	70.09	70.69	-[c]	60.9	
L	α-1,2-Man*p* [b]	5.14	4.02	3.87	3.66	3.79	3.67	3.81
		100.61	78.09	70.09	70.69	-	60.9	
M	α-1,2,6-Man*p*	5.03	3.95	3.89	3.61	-	3.70	3.86
		98.16	78.63	70.14	69.50	-	65.43	
N	α-T-Man*p*	4.96	3.99	3.76	3.57	3.68	3.68	3.80
		102.22	69.91	70.67	66.91	73.14	60.91	
O	β-T-Gal*f*	5.04	4.06	4.00	4.01	-	-	-
		105.78	81.07	76.62	82.84	-	-	

535 [a] the residue was linked with →2,6)- α-D-Manp-(1→

536 [b] the residue was linked with →2)- α-D-Manp-(1→

537 [c] not obtained due to low resolution.

538